Synthesis, calorimetric studies, and crystal structures of *N*, *O*-diacylethanolamines with matched chains[S]

Ravi Kanth Kamlekar,[1] Pradip K. Tarafdar,[1] and Musti J. Swamy[2]

School of Chemistry, University of Hyderabad, Hyderabad-500 046, India

Abstract **Recent studies show that *N*-, *O*-diacylethanolamines (DAEs) can be derived by the *O*-acylation of *N*-acylethanolamines (NAEs) under physiological conditions. Because the content of NAEs in a variety of organisms increases in response to stress, it is likely that DAEs may also be present in biomembranes. In view of this, a homologous series of DAEs with matched acyl chains (n = 10–20) have been synthesized and characterized. Transition enthalpies and entropies obtained from differential scanning calorimetry show that dry DAEs with even and odd acyl chains independently exhibit linear dependence on the chainlength. Linear least-squares analyses yielded incremental values contributed by each methylene group to the transition enthalpy and entropy and the corresponding end contributions. *N*-, *O*-Didecanoylethanolamine (DDEA), *N*-, *O*-dilauroylethanolamine (DLEA), and *N*-, *O*-dimyristoylethanolamine (DMEA) crystallized in the orthorhombic space group Pbc_{21} with four symmetry-related molecules in the unit cell. Single-crystal X-ray diffraction studies show that DDEA, DLEA, and DMEA are isostructural and adopt an L-shaped structure with the *N*-acyl chain and the central ethanolamine moiety being essentially identical to the structure of *N*-acylethanolamines, whereas the *O*-acyl chain is linear with all-trans conformation. In all three DAEs, the lipid molecules are organized in a bilayer fashion wherein the *N*-acyl and *O*-acyl chains from adjacent layers oppose each other.—** Kamlekar, R. K., P. K. Tarafdar, and M. J. Swamy. **Synthesis, calorimetric studies, and crystal structures of *N*, *O*-diacylethanolamines with matched chains. *J. Lipid Res.* 2010.** 51. **42–52.**

Supplementary key words ethanolamine • hydrogen bonding • differential scanning calorimetry • single-crystal X-ray diffraction • chain packing • bilayer structure

Ethanolamine is a central building block in a number of important membrane phospholipids and other amphiphiles. Diacyl phosphatidylethanolamine, dialkyl phosphatidylethanolamine, and phosphatidylethanolamine plasmalogen are some of the membrane lipids that contain ethanolamine. In addition, choline, which is partly derived by the progressive methylation of ethanolamine in certain tissues such as liver and brain (1, 2), is present in phosphatidylcholine, sphingomyelin, and platelet-activating factor (PAF). Besides these well-known membrane phospholipids, ethanolamine is also a structural component of *N*-acylethanolamines (NAEs) and *N*-acylphosphatidylethanolamines (NAPEs), which are present in a wide variety of organisms and whose content increases in the parent organisms when they are subjected to different types of stress, suggesting that they may take part in stress-combating responses of the parent organisms (3, 4). In addition to their putative role in combating stress, NAEs also exhibit interesting biological and medicinal properties. It has been shown that *N*-arachidonylethanolamine (anandamide) acts as an endogenous ligand of type-1 cannabinoid receptors, inhibits gap-junction conductance, and reduces the fertilizing capacity of sperm (5–7), whereas *N*-palmitoylethanolamine acts as an agonist for the type-2 cannabinoid receptor (8). *N*-myristoylethanolamine (NMEA) and *N*-lauroylethanolamine are secreted into the culture medium of tobacco cells when challenged by the fungal elicitor xylanase (9). Because of the diverse biological activities exhibited by them and in view of their putative roles in

This work was supported by the Centre for Nanotechnology established by the Department of Science and Technology (India) at the University of Hyderabad in which M.J.S. is a co-investigator. R.K.K. and P.K.T. were supported by Senior Research Fellowships from Coucil of Scientific and Industrial Research (India). Use of the National Single Crystal Diffractometer Facility (SMART APEX CCD single crystal X-ray diffractometer) at the School of Chemistry, University of Hyderabad, funded by the Department of Science and Technology (India) is gratefully acknowledged. We thank the University Grants Commission (India) for their support through the University with Potential for Excellence and Center for Advanced Research programs, to the University of Hyderabad and School of Chemistry, respectively.

Manuscript received 6 March 2009 and in revised form 9 July 2009.

Published, JLR Papers in Press, July 13, 2009
DOI 10.1194/jlr.M900105-JLR200

Abbreviations: DAE, *N*-,*O*-diacylethanolamine; DDEA, *N*-, *O*-didecanoylethanolamine; DLEA, *N*-, *O*-dilauroylethanolamine; DMEA, *N*-, *O*-dimyristoylethanolamine; DSC, differential scanning calorimetry; NAE, *N*-acylethanolamine; NAPE, *N*-acylphosphatidylethanolamine; NMEA, *N*-myristoylethanolamine; NPEA, *N*-palmitoylethanolamine; NSEA, *N*-stearoylethanolamine; T_t, transition temperature; ΔH_t, transition enthalpies; ΔS_t, transition entropies; ΔH_{inc}, incremental enthalpy; ΔS_{inc}, incremental entropy; ΔH_o, end contribution of enthalpy; ΔS_o, end contribution of entropy.

[1] These two authors contributed equally to this study.
[2] To whom correspondence should be addressed.
e-mail: mjssc@uohyd.ernet.in or mjswamy1@gmail.com

[S] The online version of this article (available at http://www.jlr.org) contains supplementary data.

combating stress and signaling events in animals and plants, several groups including ours have investigated the biophysical properties of NAPEs and NAEs and characterized their interaction with other membrane lipids (10–19).

NAEs can be further derivatized via the hydroxy group, and a recent study reported the occurrence of phosphorylcholine derivatives of NAEs in vivo (20). Also, *O*-aryloxyacetyl derivatives of NAEs have shown better plant growth stimulating effect than NAEs (21). It has also been reported that rat heart cell-free preparations can catalyze *O*-acylation of NAEs in the presence of fatty acid and acyl-CoA-generating cofactors to produce *N*-, *O*-diacylethanolamines (DAEs) (3). In another study, it was shown that lipases can catalyze *O*-acylation of *N*-acylethanolamines to yield DAEs (22). These observations suggest that DAEs may be present in biological membranes as minor constituents, which may play some biological role in the parent organisms. In order to understand the possible role played by DAEs, it is essential to investigate the properties of these molecules in a systematic manner. Particularly, studies aimed at understanding the phase behavior and structures formed by them in the solid state as well as in the fully hydrated state will be of great value in understanding their biological implications in the parent organism. In the present study, we report the synthesis of a homologous series of DAEs of matched acyl chainlengths and their characterization by IR and NMR spectroscopy. The thermotropic phase transitions of DAEs with matched *N*- and *O*-acyl chainlengths (n = 10–20) have been characterized by differential scanning calorimetry (DSC). Finally, the 3-dimensional structure of three compounds from this series, namely *N*-, *O*-didecanoylethanolamine (DDEA), *N*-, *O*-dilauroylethanolamine (DLEA), and *N*-, *O*-dimyristoylethanolamine (DMEA) have been investigated by single-crystal X-ray diffraction and the molecular packing and intermolecular interactions in the crystal lattice have been analyzed.

MATERIALS AND METHODS

Materials

Long-chain fatty acids, CH_3-$(CH_2)_n$-COOH, of even and odd chain lengths (n = 8–18) were purchased from Aldrich. Oxalyl chloride was obtained from Merck (Germany). Ethanolamine and other solvents were purchased locally.

Synthesis of DAEs

DAEs of matched acyl chains were synthesized by the reaction of acid chlorides with 2-ethanolamine. For this, long-chain fatty acids were converted to the corresponding acid chlorides by treating with 4 mol equivalents of oxalyl chloride at room temperature for 2 h under nitrogen atmosphere (10). After completion of the reaction, the excess oxalyl chloride was removed under a stream of dry nitrogen gas. DAEs were synthesized by the drop-wise addition of about 2.5 mol equivalents of the acid chloride in dichloromethane to a solution of 1 mol equivalent of freshly distilled 2-ethanolamine in dichloromethane in an ice bath under constant stirring. After all the reagent was added, the reaction was allowed to continue overnight (**Scheme 1**). The reaction mixture was then washed twice with double distilled water and extracted with ether and then the organic solvent was evaporated under a stream of dry nitrogen gas. The crude products were purified by column chromatography on silica gel. Elution was done by using an increasing concentration of ethyl acetate in n-hexane. The product obtained was concentrated and was dissolved in a small amount of dichloromethane, and about 10 vol of acetone was added to it and the solution was kept in a freezer (ca. −20°C) overnight. This led to the precipitation of the DAEs, which were recovered by filtration. Yields ranged between 55% and 60%. The purified products were characterized by IR and ^{1}H-NMR spectroscopy (See supplementary data online).

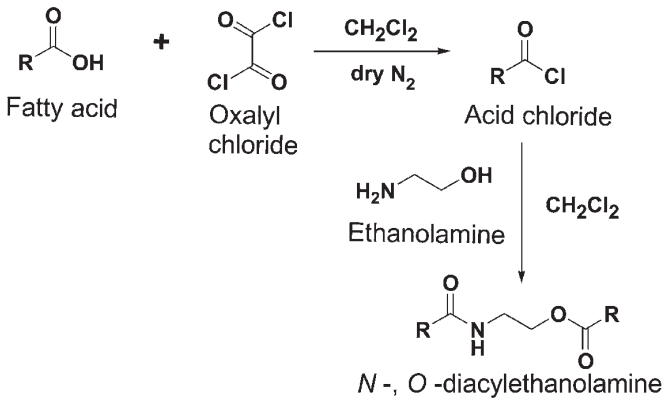

Scheme 1. Synthesis of N, O-diacylethanolamine.

DSC

DSC studies were carried out on a Perkin-Elmer PYRIS Diamond differential scanning calorimeter on DAEs that were obtained by recrystallization from dichloromethane/acetone mixture at −20°C. Samples of dry DAEs (1–3 mg) were weighed accurately into aluminum sample pans, covered with an aluminum lid and sealed by crimping. Reference pans were prepared similarly but without any sample in them. Heating and cooling scans were performed from room temperature (ca. 25°C) to about 110°C at a scan rate of 1.0°/min or 2.0°/min and each sample was subjected to two heating scans and one cooling scan. Transition enthalpies were determined by integrating the peak area under the transition curve. In all cases, only the first heating scan was considered for further analysis. Transition entropies were determined from the transition enthalpies assuming a first order transition according to the expression (23):

$$\Delta H_t = T.\Delta S_t \qquad \textit{(eq. 1)}$$

where T is transition temperature and ΔH_t values are taken at this temperature in order to calculate the corresponding ΔS_t values.

Capillary melting points of the compounds were recorded on a Superfit (Mumbai, India) capillary melting apparatus. Briefly, the solid sample was packed in a glass capillary with one end sealed and the melting of compound was monitored visually by means of a magnifying lens, which was built into the apparatus. Temperature was measured to ± 0.1 degree accuracy with a calibrated thermometer provided with the apparatus.

Crystallization, X-ray diffraction, and structure solution

Thin plate type, colorless crystals of DDEA, DLEA, and DMEA were grown at room temperature from a 1:1 (v/v) mixture of dichloromethane and a trace of methanol. X-ray diffraction measurements were carried out at room temperature (ca. 25°C) with

a Bruker SMART APEX CCD area detector system using a graphite monochromator and Mo-Kα (λ = 0.71073 Å) radiation obtained from a fine-focus sealed tube. The minimum resolution of X-ray diffraction measurement is 0.84 Å. Data reduction was done using Bruker SAINTPLUS program. Absorption correction was applied using SADABS program and refinement was done using SHELXTL program (24). The crystal parameters for all the three compounds are presented in **Table 1**.

Lattice energy calculations

Lattice energy calculations of DDEA, DLEA, and DMEA were performed using the COMPASS force field in Cerius[2] suite of programs (Accelrys Inc., San Diego, CA). Lattice energies were reported after normalizing the values obtained for a single molecule.

RESULTS AND DISCUSSION

Synthesis and characterization of DAEs

DAEs of matched acyl chainlengths (n = 10–20) have been synthesized in fair yields by the reaction of the corresponding acid chlorides with 2-ethanolamine. The DAEs, purified by column chromatography and recrystallization (from dichloromethane –acetone mixture at −20°C), were found to be pure by thin-layer chromatography. Infrared spectra (KBr pellet) of the recrystallized DAEs contained absorption bands due to the amide linkage at 1645–1639 cm^{-1} (amide-I) and 1553–1543 cm^{-1} (amide-II) and at 1738–1734 cm^{-1} due to the ester carbonyl. The amide N−H stretching is seen at 3319–3301 cm^{-1}, whereas C−O stretching from the ester moiety is observed around 1188–1178 cm^{-1}. Methylene bending and rocking bands were observed near 1470 cm^{-1} and 720 cm^{-1}. Most of the DAEs except didecanoylethanolamine, diundecanoylethanolamine, and ditridecanoylethanolamine exhibit split bands corresponding to the methylene bending (1470 cm^{-1}) and rocking (720 cm^{-1}), which is characteristic of $O_{\perp}$ chain packing (25–27). Even though the splitting of these bands is not clearly seen for didecanoylethanolamine, diundecanoylethanolamine, and ditridecanoylethanolamine, the bands are relatively broad and are likely to be composed of two peaks. These observations suggest that the chain packing among the DAEs with different acyl chains investigated here are similar. The specific band positions for these and other absorptions such as C−H symmetric and asymmetric stretching are listed in supplementary Table I. ^{1}H-NMR spectra of DAEs were recorded on a Bruker Avance 400 MHz NMR spectrometer using $CDCl_3$ as the solvent. A representative ^{1}H-NMR spectrum corresponding to dipentadecanoylethanolamine is shown in supplementary Fig. XII. Results of ^{1}H-NMR spectra for the different DAEs investigated in this study together with assignments are given in supplementary Table II.

TABLE 1. Crystallographic data for *N*-, *O*-diacylethanolamines at 298 K

Compound	DDEA	DLEA	DMEA
Formula	$C_{22}H_{43}NO_3$	$C_{26}H_{51}NO_3$	$C_{30}H_{59}NO_3$
Formula wt.	369.6	425.68	481.78
Crystal system	orthorhombic	orthorhombic	orthorhombic
Space group	Pbc_{21}	Pbc_{21}	Pbc_{21}
a (Å)	4.8725(6)	4.8756(4)	4.8949(9)
b (Å)	9.0827(11)	8.7865(8)	9.0411(16)
c (Å)	53.033(6)	60.300(5)	69.773(12)
Z	4	4	4
V (Å^3)	2347.0(5)	2583.2(4)	3087.8(10)
D_{calc} (g cm^{-3})	1.046	1.095	1.036
R1	0.0566	0.0621	0.0769
wR2	0.1491	0.1580	0.2010
GooF	0.973	1.175	1.039

R1 = $\Sigma \mid \mid F_o \mid - \mid F_c \mid \mid / \Sigma \mid F_o \mid$, wR2 = $\{ \Sigma [w(F_o^2 - F_c^2)^2] / \Sigma [w(F_o^2)^2] \}^{1/2}$, GooF (Goodness of fit) = S = $\{ \Sigma [w(F_o^2 - F_c^2)^2] / (n - p) \}^{1/2}$ where F_o is observed intensity, F_c is calculated intensity, w is weight factor, n is the number of reflections and p is the total number of parameters refined. R1 and wR2 represents the convergence of the refinement. The lower the value, the better fitting of parameters.

DSC of dry DAEs

Heating thermograms corresponding to dry DAEs of even matched acyl chainlengths are shown in **Fig. 1A** and those corresponding to DAEs with matched odd acyl chainlengths are shown in Fig. 1B. The corresponding cooling scans are shown in **Fig. 2A** and Fig. 2B, respectively. Whereas the heating scans gave endothermic transitions, the cooling scans yielded exothermic transitions. The heating thermograms presented in Fig. 1A and Fig. 1B show that each DAE exhibits a major transition and this transition was found to correspond to the capillary melting point of the compound. Some of the DAEs also show one or two additional minor transitions at lower temperatures and the multiple transitions are reproducible for samples obtained from different batches. These transitions, therefore, must correspond to solid-solid phase transitions and indicate the possibility of polymorphism. When the samples were subjected to a second heating scan, it was observed that the additional transitions disappear in some cases and small decreases have been noted in the transition enthalpies. This suggests that during cooling scan

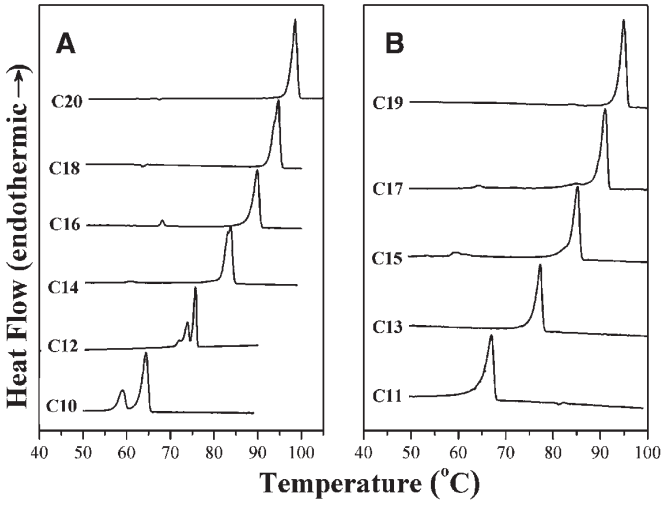

Fig. 1. DSC heating thermograms of *N*-, *O*-diacylethanolamines. A: Thermograms of DAEs with even number of C-atoms in the acyl chains. B: Thermograms of DAEs with odd number of C-atoms in the acyl chains. The number of C-atoms in the acyl chain is indicated against each thermogram.

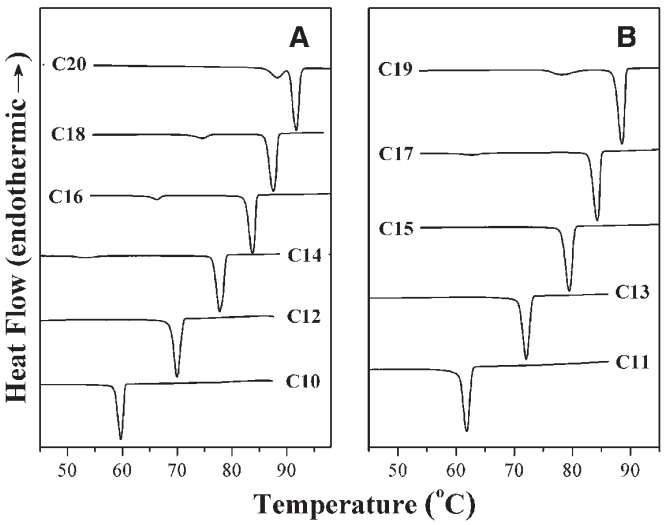

Fig. 2. DSC cooling thermograms of *N*-, *O*-diacylethanolamines. A: DAEs with even number of C-atoms in the acyl chains, B: DAEs with odd number of C-atoms in the acyl chains. The number of C-atoms in the acyl chain is indicated against each thermogram.

some of the DAEs do not come back to the structure of initial starting form. Therefore, in all cases, only the first heating scan was considered for further analysis and the total area under the major and minor transitions was integrated to get the transition enthalpies. The transition temperatures (T_t), transition enthalpies (ΔH_t), and transition entropies (ΔS_t) obtained from the first heating thermograms and the corresponding cooling thermograms are presented in **Table 2**. It is clearly seen from the data presented in this table that the transition temperatures obtained from the cooling thermograms are several degrees lower as compared with heating thermograms; that is, the thermograms display hysterisis, which is due to relatively faster scan rate.

When the DSC scans were run with *N*-, *O*-dipalmitoylethanolamine in the presence of excess water, the thermograms obtained were essentially identical to those obtained with the dry samples, suggesting that the chain melting phase transitions of DAEs with long matched acyl chains are not affected by the presence of water. As DAEs have no major polar groups, it is unlikely that water easily penetrates the crystalline lattice. The hydration of polar head group generally reduces the chain melting transition temperature. For example, it was observed that phosphatidylcholines, which contain a more polar head group than diacylglycerols, have a lower chain melting temperature in the hydrated state (28). Similarly, in *N*-acylethanolamines with long acyl chains, hydration results in a decrease in the phase transition temperatures (13, 19), whereas the present results show that derivatization of the hydroxy group in NAEs by attaching a long acyl chain reduces the polarity of the head group region significantly, which completely eliminates interaction of the lipid with water. In view of this, no further DSC studies were conducted with the DAEs in the presence of water.

Chainlength dependence of transition enthalpy and transition entropy

The chainlength dependence of transition enthalpy and transition entropy for the chain-melting phase transitions of DAEs of matched *N*- and *O*-acyl chainlengths are given in **Fig. 3A** and 3B, respectively. In both cases, it is observed that the even and odd series independently exhibit linear dependence of the calorimetric parameters on the acyl chainlength. However, when the data obtained with the even and odd chainlength series are viewed together, a zig-zag pattern is seen, with the values of enthalpy and entropy for the odd chainlength series being slightly lower than those of the even chainlength series. In other words, the calorimetric data exhibit even-odd alternation and this aspect will be discussed in more detail below. The enthalpy and entropy data for DAEs of matched, even, and odd acyl chainlegths could be fit well to expressions 2 and 3 given below (29), as observed earlier for NAEs with even and odd acyl chainlengths (13, 30):

$$\Delta H_t = \Delta H_o + (n-2)\Delta H_{inc} \qquad \textit{(eq. 2)}$$

$$\Delta S_t = \Delta S_o + (n-2)\Delta S_{inc} \qquad \textit{(eq. 3)}$$

where n is the number of C-atoms in the acyl chains and ΔH_o and ΔS_o are the end contributions to ΔH_t and ΔS_t, respectively, arising from the terminal methyl groups and

TABLE 2. Transition temperatures (T_t), transition enthalpies (ΔH_t), and transition entropies (ΔS_t) associated with the solid-liquid phase transition of *N*-, *O*-diacylethanolamines with matched acyl chainlengths

Acyl Chainlength (n)	T_t (°C)	ΔH_t (kcal.mol^{-1})	ΔS_t (cal.mol^{-1}.K^{-1})
C_{10}	64.0 ± 0.55 (59.6 ± 0.67)	15.1 ± 0.28 (10.9 ± 0.27)	44.8 (32.8)
C_{11}	66.9 ± 0.55 (61.8 ± 0.60)	12.8 ± 0.09 (10.8 ± 0.28)	37.7 (32.2)
C_{12}	75.6 ± 0.78 (70.6 ± 1.00)	18.2 ± 0.50 (13.6 ± 0.71)	52.2 (39.7)
C_{13}	76.7 ± 0.06 (72.2 ± 0.55)	16.9 ± 0.31 (14.3 ± 0.27)	48.3 (41.4)
C_{14}	83.6 ± 0.20 (78.8 ± 1.05)	22.5 ± 0.04 (19.4 ± 0.19)	63.1 (55.1)
C_{15}	84.9 ± 0.52 (80.0 ± 0.49)	20.3 ± 0.85 (16.8 ± 0.17)	56.7 (47.6)
C_{16}	89.9 ± 0.40 (84.8 ± 0.36)	26.4 ± 0.74 (22.2 ± 0.80)	72.7 (62.0)
C_{17}	91.2 ± 0.36 (85.5 ± 0.21)	25.5 ± 0.31 (23.4 ± 1.34)	70.0 (65.3)
C_{18}	94.6 ± 0.37 (88.9 ± 0.99)	29.2 ± 0.12 (25.1 ± 0.30)	79.4 (69.3)
C_{19}	94.8 ± 0.29 (89.4 ± 0.26)	28.3 ± 0.18 (26.1 ± 0.15)	76.9 (72.0)
C_{20}	98.7 ± 0.17 (91.6 ± 0.36)	33.6 ± 1.02 (32.9 ± 0.23)	90.6 (90.2)

Average values from three independent measurements are shown along with standard deviations. Values given in parentheses correspond to data obtained from cooling scans.

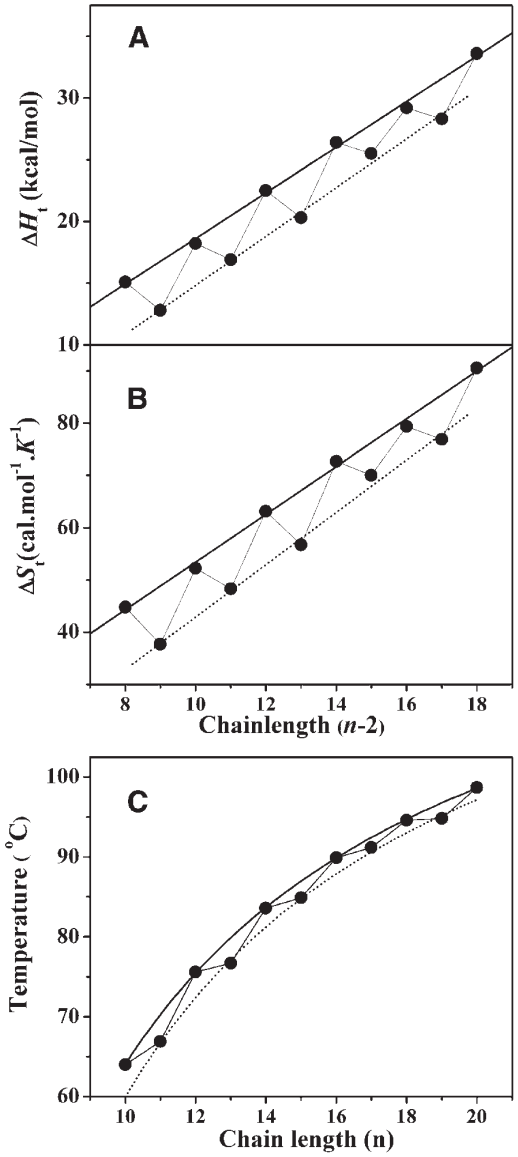

Fig. 3. Chainlength dependence of transition enthalpies (ΔH_t), transition entropies (ΔS_t), and transition temperatures (T_t). Transition enthalpies (A) and transition entropies (B) obtained for the thermotropic phase transitions of *N*-, *O*-diacylethanolamines of matched acyl chainlengths are plotted against the number of methylene units (n−2, where n is the number of C-atoms) in each acyl chain. C: Chainlength dependence of phase transition temperatures of *N*-, *O*-diacylethanolamines of matched acyl chainlengths, showing even-odd alternation. Solid and dotted lines correspond to nonlinear least squares fits of the transition temperatures of even-chainlength and odd-chainlength series to equation 7.

the central polar region of the DAE molecule. ΔH_{inc} and ΔS_{inc} are the incremental values of ΔH_t and ΔS_t contributed by two CH_2 groups (one from the *N*-acyl chain and the other from the *O*-acyl chain). Linear least-squares analysis of the chainlength-dependent values of ΔH_t and ΔS_t for the even and odd series DAEs yielded the incremental values (ΔH_{inc} and ΔS_{inc}) and end contributions (ΔH_o and ΔS_o), which are listed in **Table 3**. A linear chainlength dependence of the transition enthalpy and transition entropy observed here for the DAEs of even chainlengths and odd chainlengths indicates that structures of the DAEs of different even and odd chainlengths are very similar in the solid state and the liquid state. This suggests that the molecular packing and hydrogen bonding patterns in all the even chainlength DAEs are likely to be very similar, and determination of the 3-dimentional structure of any one DAE with matched acyl chains is likely to give an idea of the molecular packing and intermolecular interactions present in the crystal for the entire homologous series. In the present study, three different DAEs with matched acyl chains have been shown to be isostructural (see below), which strongly suggests that all the DAEs investigated are also likely to have very similar molecular packing and intermolecular interactions.

The ΔH_{inc} values of 1.84 and 1.98 kcal.mol^{-1} observed here for the DAEs with even and odd chainlengths, respectively, correspond to the contribution of two acyl chains and in order to obtain the average contribution of each CH_2 group, these values should be halved. The corresponding per-chain ΔH_{inc} values would then be 0.92 and 0.99 kcal.mol^{-1}, respectively, for the DAEs with even and odd chainlengths. A comparison of these values with the corresponding values obtained previously for the NAEs shows that the incremental enthalpy contributed by each CH_2 unit in the DAEs is higher than that observed with the NAEs. The ΔS_{inc} values obtained here for the DAEs with matched acyl chainlengths (the per-chain values being 2.28 and 2.50 J.mol^{-1}.K^{-1}, for the even and odd chainlength series, respectively) are also considerably higher than the ΔS_{inc} values obtained for the NAEs (13, 30). These two factors, taken together, suggest that the change in the order resulting from the chain melting phase transition is higher for the DAEs than the NAEs and indicate that acyl chains in DAEs are packed more tightly.

Chainlength dependence of transition temperatures

Although the data presented in Table 2 show that the transition temperatures increase with increasing acyl chainlength, the increase in the transition temperature (T_t) is not linearly proportional to the acyl chainlength. In order to understand this better, the transition temperatures were plotted as a function of acyl chainlength (Fig. 3C). From this figure it is apparent that the T_t values exhibit an even-odd alternation, with the even chainlength series exhibiting somewhat higher transition temperatures than the odd chainlength compounds. This aspect is discussed in more detail below. Within each series, however, the T_t values increase in a smooth progression but with decreasing increments as the chainlength is increased. As the acyl chainlength increases, the total contribution from the polymethylene portion toward the total enthalpy and entropy of the phase transition will be sufficiently large that the end contributions are negligible in comparison. At infinite acyl chainlength, equations 2 and 3 can be reduced to (13):

$$\Delta H_t = (n-2)\Delta H_{inc} \qquad \textit{(eq. 4)}$$

$$\Delta S_t = (n-2)\Delta S_{inc} \qquad \textit{(eq. 5)}$$

TABLE 3. Incremental values (ΔH_{inc}, ΔS_{inc}) of chain length dependence and end contributions (ΔH_o, ΔS_o) to phase transition enthalpy and entropy of dry *N*-, *O*-diacylethanolamines

Lipid	ΔH_{inc}	ΔH_o	ΔS_{inc}	ΔS_o
DAEs (even chainlength)	1.84 (± 0.04)	0.13 (± 0.66)	4.57 (± 0.14)	7.67 (± 1.88)
DAEs (odd chainlength)	1.98 (± 0.09)	−4.98 (± 1.19)	5.00 (± 0.24)	−7.14 (± 3.22)

Average values of transition enthalpy and transition entropy given in Table 2 have been used for the linear fitting of the data. Errors shown in parentheses are fitting errors obtained from the linear least-squares analysis.

Then the transition temperature for infinite chainlength, T_t^{∞}, will be given by:

$$T_t^{\infty} = \Delta H_{inc}/\Delta S_{inc} \qquad \textit{(eq. 6)}$$

From the data presented in Table 3, the T_t^{∞} values for the DAEs of even and odd chainlengths have been estimated as 402.6 and 396.0 K, respectively.

The chainlength dependence of the transition temperatures of DAEs of both even and odd acyl chainlengths was fitted to equation 7, predicted from the linear dependence of transition enthalpy and transition entropy given in equations 2 and 3 (23, 31, 32):

$$T_t = \Delta H_t/\Delta S_t = T_t^{\infty}\left[1 - \left(n_o - n_o'\right)/\left(n - n_o'\right)\right] \qquad \textit{(eq. 7)}$$

where n_o (= $-\Delta H_o/\Delta H_{inc}$) and n_o' (= $-\Delta S_o/\Delta S_{inc}$) are the chainlengths at which the transition enthalpy and transition entropy, respectively, extrapolate to zero. From the nonlinear least-squares fits shown in Fig. 3C, it is evident that the transition temperatures of DAEs with even and odd chainlengths are described accurately by equation 7. In addition, the fitting parameters yielded the transition temperature at infinite chainlength (T_t^{∞}) for the DAEs of matched even and odd acyl chains as 407.2 K with χ^2 of 0.02 and 407.2 K with χ^2 of 0.38, respectively. These values are in good agreement with the values estimated from the linear regression analysis of the calorimetric data, discussed above.

Even-odd alternation in transition temperatures and thermodynamic parameters

It is interesting to note that the phase transition temperatures and thermodynamic parameters (ΔH_t and ΔS_t) for DAEs exhibit an even-odd alternation. Similar trends were observed in the transition temperatures and physical properties of long-chain hydrocarbons, fatty acids, and *N*-acylethanolamines in the solid phase, as well as for the chain melting phase transition temperatures of NAEs in the hydrated state (13, 29). Such alternation has been explained on the basis of packing of the hydrocarbon chains. In long-chain fatty acids, for example, it was shown by Larsson (29) that differences in the packing properties between the terminal methyl groups between the even and odd members can explain the differences in the physical properties. Such differences do not arise in the methyl group packing if the chains are perpendicular to the methyl group plane. However, when the hydrocarbon chains are tilted with respect to the plane of the methyl groups, their packing modes can differ, leading to alternation in the physical properties. The even-odd alternation in the transition temperatures, enthalpies, and entropies of DAEs of matched acyl chainlengths is consistent with the tilted *N*- and *O*-acyl chains observed in the crystal structure of DDEA, DLEA, and DMEA, discussed below.

Description of the structure

The molecular structure of DLEA is shown in the ORTEP plot given in **Fig. 4**, along with the atom numbering for all the nonhydrogen atoms. The atomic coordinates and equivalent isotropic displacement parameters for all nonhydrogen atoms and the hydrogen atom on the heteroatom (N−H) are given in supplementary Table III. The bond distances and bond angles involving all the nonhydrogen atoms are given in supplementary Table IV and the corresponding torsion angles are given in supplementary Table V. It is clearly seen from Fig. 4 that the hydrocarbon portions of the two acyl chains (C12−C1, corresponding to the

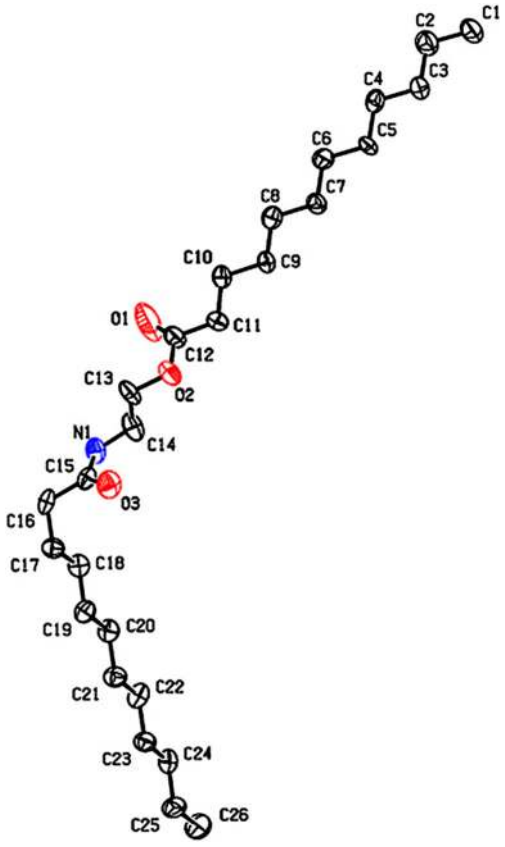

Fig. 4. ORTEP plot showing the molecular structure of *N*-, *O*-dilauroylethanolamine (DLEA).

O-acyl chain and C17−C26, corresponding to the *N*-acyl chain) of the molecule are in all-*trans* conformation. The torsion angle observed for acyl chain region, excepting the C15−C16−C17−C18 angle, which is −67.7°, are all close to 180° and are fully in agreement with the above observation. The gauche conformation at the C16-C17 bond results in a bending of the molecule, giving it an 'L' shaped conformation with both acyl chains coming off the two ends of the ethanolamine moiety. The two chains of the L-shaped molecule are oriented at an angle of 110° with respect to each other. The carbonyl group and the amide N−H are also in *trans* geometry. The conformation of the *N*-acyl chain and the central ethanolamine moiety in DLEA are essentially identical to that observed in the crystal structures of *N*-palmitoylethanolamine, *N*-myristoylethanolamine, and *N*-stearoylethanolamine (33–35). Thus, esterification of the hydroxyl group of NAE to produce *N*-, *O*-diacylethanolamine does not seem to affect the conformation of the *N*-acyl region.

DDEA and DMEA are isostructural with DLEA and the ORTEP plots of the compounds are given in supplementary figs. XIII and XIV. The atomic coordinates and equivalent isotropic displacement parameters of selected atoms, bond angles, bond length, and torsion angles of the two molecules are presented in supplementary Tables VI–XI. The C13−C14−C15−C16 torsion angle in DDEA is found to be −69.0°, whereas the C17-C18-C19-C20 torsion angle in DMEA is −68.8°. Both the DAEs also adopt an 'L' shape in the solid state due to the gauche conformation at the C14-C15 bond in DDEA and C18-C19 in DMEA. The two acyl chains coming off the two ends of the ethanolamine moiety make an angle of 113.1° with each other in DDEA and 112.2° in DMEA. In all the three molecules, the torsion angle at gauche conformation is very similar and the angle of intersection of the two acyl chains is also nearly identical.

Molecular packing

Packing diagrams of DLEA along the *b*-axis and the *a*-axis are given in **Fig. 5A** and B, respectively. The DLEA molecules are packed in layers that are stacked in such a way that the methyl groups of the *O*-acyl chains from one layer face the methyl groups of the *N*-acyl chains of the layer above it. The methyl ends of the stacked bilayers are in van der Waals' contacts with the closest methyl-methyl distance between opposite layers and the same layer being 3.882 Å and 4.876 Å, respectively. The layer thickness (C1−C26 distance) in the crystal structure of DLEA is 27.82 Å and the all-*trans* *N*- and *O*-acyl chains of the molecule are tilted by 36.5° and 34.5°, respectively, with respect to the normal to the respective methyl end planes. These values are in the same range as the tilt angles with respect to the bilayer normal found in NMEA, *N*-palmitoylethanolamine (NPEA), and *N*-stearoylethanolamine (NSEA) (35–37°) (33–35). Other long chain molecules such as long chain carboxylic acids and n-alcohols also pack in a bilayer form with tail-to-tail hydrocarbon alignment with tilted chains (29). In the bilayer stack, the *N*-lauroyl chain packs in one layer, the *O*-lauroyl chain in the other, which

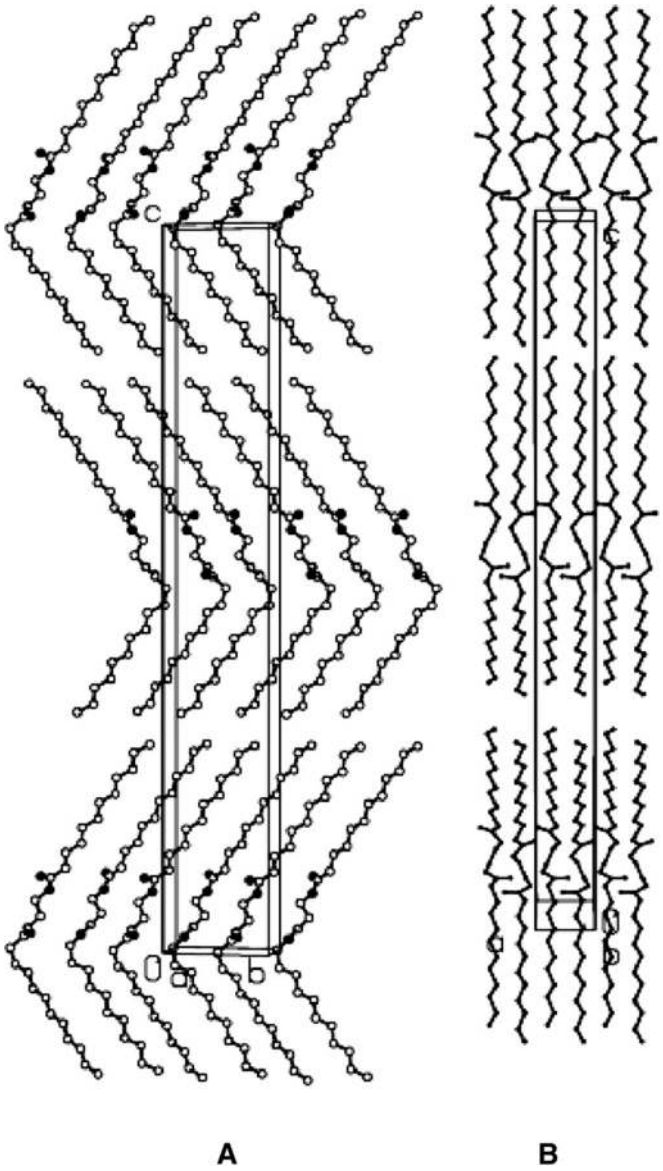

Fig. 5. Packing diagrams of DLEA. A: A view along with *b*-axis. B: A view along with *a*-axis.

results in a mixed bilayer arrangement with no mixing of *N*-lauroyl and *O*-lauroyl chains in one layer. The molecular packing is very similar to that observed in the crystal structures of 1,3 diacylglycerols (36) and *N*-tetracosanoylphytosphingosine (37), which belongs to the class of compounds known as ceramides. Similar packing of acyl chains, where both chains are segregated from the head group, has been reported in hydrated 1-stearoyl, 2-arachidonylglycerol (38). The molecular packing is different from that observed in saturated 1,2 diacylglycerols (39, 40), where the chain in the primary position bends at the carbonyl so that it forms a hairpin conformation and lies next to the sn-2 chain.

Packing arrangement in the crystal structures of DDEA and DMEA (supplementary figs. XV and XVI) are very similar to that seen in DLEA, described above. Molecules of DDEA and DMEA are packed in the crystal lattice in layers that are stacked in such a way that the methyl groups of the

O-acyl chains from one layer face the methyl groups of the *N*-acyl chains of the layer above it. The methyl ends of the stacked bilayers are in van der Waals' contacts in DDEA, with the closest methyl-methyl distance between opposite layers and the same layer being 3.93 Å and 4.87 Å, respectively. The layer thickness (C1−C22 distance) in DDEA is 24.07 Å and the all-*trans N*- and *O*-acyl chains of the molecule are tilted by 34.6° and 31.8°, respectively, with respect to the normal to the respective methyl end planes. Similarly, in DMEA, the closest methyl-methyl distances between the opposite layers and the same layer are 3.93 Å and 4.89 Å, respectively. The layer thickness (C1−C30 distance) in DMEA is 32.39 Å and the all-*trans N*- and *O*-acyl chains of the molecule are tilted by 34.6° and 33.2°, respectively, with respect to the normal to the respective methyl end planes.

The packing coefficient for DLEA is 68.5%, which is higher than the values observed for NSEA (65.2%), NPEA (65.3%), and NMEA (55%). Packing coefficient of DMEA is 64.9%, which is also higher than its precursor NMEA. For DDEA, the calculated packing coefficient is 64.1%. These results suggest that the acyl chains in DAEs are packed more tightly than in NAEs.

Molecular area

The area per molecule in the plane of the bilayer for DDEA, DLEA, and DMEA obtained from the corresponding crystal structures are 22.12, 21.42, and 22.13 $Å^2$, respectively. These values are in the same range as the values of molecular area found for the NAEs whose 3-dimensional structures have been determined earlier, namely NPEA (21.99 $Å^2$ and 22.03 $Å^2$ for polymorphs α and β, respectively), NMEA (21.95 $Å^2$), and NSEA (21.99 $Å^2$), as well as some other two-chain lipids such as 2,3-dilauroyl-D-glycerol, 1,2-dipalmitoyl-sn-glycerol, and 1-strearoyl-3-oleoyl-glycerol, whose molecular areas are in the range of 20.0-25.7 $Å^2$ (33–36, 39, 40).

Subcell structure

The different lateral packing modes adopted by hydrocarbon chains in lipid crystals are generally described by subcells that specify the relations between equivalent positions within the chain and its neighbors. From an analysis of a large number of lipid crystal structures, it was shown that such chain packing modes fall into a relatively small number of hydrocarbon subcells with triclinic, monoclinic, orthorhombic, and hexagonal symmetry and that their polymethylene planes can be mutually parallel or perpendicular with respect to their neighbors (41, 42). The subcells have been further divided into simple and hybrid types, with the latter involving more than two different asymmetric units in a subcell. Examination of the hydrocarbon chain packing in the *N*-acyl chain and *O*-acyl chains of DDEA, DLEA, and DMEA revealed that the subcells in both these chains are of the orthorhombic type (O'⊥). The unit cell dimensions of these subcells are given in **Table 4**.

Hydrogen bonding and intermolecular interactions

The molecular packing in the crystal structure of DLEA was examined from various angles in order to understand the intermolecular interactions. The hydrogen bonding pattern observed in the crystal lattice of DLEA is shown in **Fig. 6A**. In Figs. 6B and C, pictures of the hydrogen bonding pattern viewed along the *a*-axis and *b*-axis, respectively, are shown. Figure 6B gives a view of the molecular packing together with the hydrogen bonds between the amide hydrogen and the carbonyl oxygen atoms of adjacent layers in the same leaflet of the bilayer. These N−H···O hydrogen bonds are formed between the amide N−H group of one molecule and the amide carbonyl oxygen of an adjacent DLEA molecules along the *a*-axis. The N−H and C = O groups of the amide moiety in each molecule are in *trans* geometry

TABLE 4. Subcell dimensions of *N*- and *O*-acyl chains of DAEs

	DDEA		DLEA		DMEA	
Cell axis	*N*-acyl chain	*O*-acyl chain	*N*-acyl chain	*O*-acyl chain	*N*-acyl chain	*O*-acyl chain
a (Å)	7.39	7.66	7.13	7.22	7.39	7.53
b (Å)	4.87	4.87	4.87	4.87	4.88	4.89
c (Å)	2.55	2.54	2.56	2.53	2.55	2.55
Area per chain ($Å^2$)	17.99	18.65	17.36	17.58	18.03	18.41

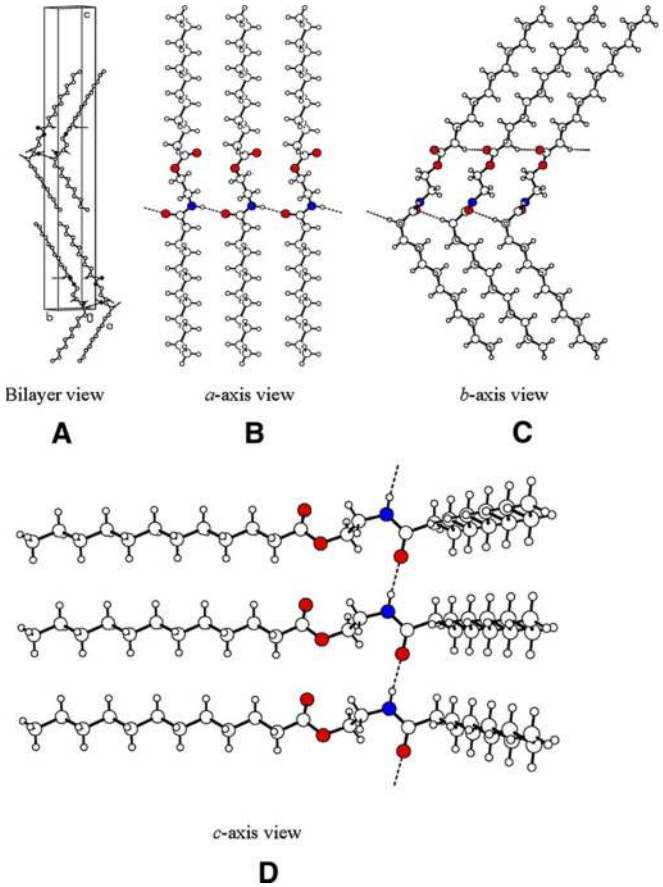

Fig. 6. Hydrogen bonding pattern in the crystal lattice of DLEA. A: A view of the bilayer displaying N-H···O type hydrogen bonding. B: A close-up view along *a*-axis displaying N-H···O type hydrogen bonding. C: A close-up view along *b*-axis displaying two C-H···O type hydrogen bonds. D: A close-up view along *c*-axis displaying N-H···O type hydrogen bonds. Symbols used are: open circle, carbon; red, oxygen; blue, nitrogen; small open circle, hydrogen.

and point in the opposite direction, thus, providing proper juxtaposition to interconnect adjacent molecules by N−H···O hydrogen bonds. All these H-bonds are identical, with an N−O distance of 2.835(5) Å, and H···O distance of 1.84 Å and an N−H···O angle of 168°. This is essentially similar to the value of 167° observed for the corresponding N−H···O angle in the crystal structure of NPEA (α polymorph) (33) and the value of 166.7° seen in NMEA (34).

In addition to the N−H···O hydrogen bonds, weak C−H···O type hydrogen bonds have been observed in the crystal structures of the three DAEs investigated here. Hydrogen bonds with interaction energies up to −5 kcal/mol are generally considered as weak hydrogen bonds (43) and many examples of weak hydrogen bonds involving C−H···O interactions have been described earlier (see, for example, refs. 44–46). Figure 6C gives a view of two C−H···O type hydrogen bonds observed in the crystal lattice of DLEA. One of these is formed between O3 (oxygen atom of the amide carbonyl group) of one molecule and one of the H-atoms on C16 (carbon atom α- to the amide carbonyl) of an adjacent molecule in the same layer. All the C−H···O hydrogen bonds between O3 and C16 are identical, with a C−O distance of 3.502(5) Å, an H···O distance of 2.42 Å, and C−H···O angle of 174°. The second C−H···O bond is formed between O1 (the ester carbonyl oxygen) of one molecule and one of the H-atoms on C11 (carbon atom α- to the ester carbonyl group) of an adjacent molecule in the same layer. All these hydrogen bonds are also identical, with a C−O distance of 3.307(7) Å, H···O distance of 2.48 Å and a C−H···O angle of 132°.

Very similar hydrogen bonding patterns have been observed in DDEA as well as in DMEA (supplementary Figs. XVII, XVIII). The H-bond distances and angles of different H-bonds observed in these two crystals are listed in supplementary Table XII.

Lattice energy calculations

Lattice energies of DDEA, DLEA, and DMEA were computed using the COMPASS force fields in the Cerius^2 program package in order to estimate their relative energies. The calculations yielded an overall energy of −59.8, −67.6, and −76.7 kcal/mol, for DDEA, DLEA, and DMEA, respectively. The calculated lattice energies from the crystal structures were found to increase linearly with acyl chainlength. Linear fit of the lattice energy yielded an intercept of −17.33 kcal/mol and slope of −4.23 kcal.mol^{-1}. chainlength^{-1} (see supplementary Fig. XIX). From the slope and intercept of linear fit, the predicted lattice energy for dipalmitoylethanolamine, distearoylethanolamine, and diarachidylethanolamine were obtained as −85.0, −93.5, and −101.9 kcal/mol, respectively. The results suggest that DAEs with long acyl chains have higher lattice energy than the DAEs having relatively short acyl chains.

Polymorphism in matched chain DAEs

DAEs with comparatively short even fatty acyl chains (DDEA, DLEA, and DMEA) exhibit relatively prominent pretransition(s) before chain-melting transition, whereas in long fatty acyl chain DAEs those prominent pretransition(s) are not seen (Fig. 1). Instead, one or two minor transitions have been observed before the main phase transition in some long acyl chains DAEs. These prominent pretransition(s) may correspond to solid-solid phase transition and suggest the possibility of solid state structural polymorphism in DAEs. It was observed that these minor as well as prominent pretransitions disappear in some cases upon second heating, which suggests that during the cooling scan those DAEs crystallize in a different polymorphic structure. The thermodynamic parameters obtained from the cooling run (Table 2) show that the ΔH_t values estimated from the cooling scan are considerably lower for DDEA and DLEA than those obtained from the first heating scan. It clearly suggests that DDEA and DLEA exist in a different polymorphic form after the cooling scan. DSC thermograms of DDEA, DLEA, and DMEA obtained from the same crop of crystals that were used for single-crystal X-ray diffraction exhibit prominent pretransition peaks that were identical to the DSC thermograms obtained from respective DAEs crystallized in dichloromethane-acetone mixture at −20°C. Therefore, it appears that the structure and packing of DAEs crystallized in dichloromethane-acetone mixture at −20°C and from dichloromethane-methanol mixture are identical. Because the stable form is often easier to crystallize, it appears that the DAEs obtained from dichloromethane-acetone mixture at −20°C correspond to the stable form. Therefore, the form obtained after the cooling scan is most likely a metastable form at room temperature.

The solid-solid phase transition mechanism is a complex phenomenon, and it is very difficult to justify why DAEs with comparatively short acyl chains exhibit prominent pretransition(s) before main phase transition. However, in view of the relatively large enthalpy involved, it appears that the prominent pretransitions involve major structural change between two polymorphic forms, for which the crystal lattice most likely has to undergo a major reorganization. Because DAEs with long acyl chains have much more lattice energy than DAEs with short acyl chains (see 'lattice energy calculations'), it requires more energy to break the crystal lattice and, therefore, they may not exhibit such prominent solid-solid phase transition.

Correlation of crystal structure and thermodynamic properties

Analysis of the crystal structure of DLEA and comparison of the subcell structures of the *N*- and *O*-acyl chains in it with those of NMEA and NPEA, discussed above, have shown that the acyl chains in DLEA are more tightly packed than those in NMEA and NPEA, with DLEA having a smaller area per chain (17.40 and 17.61 Å^2, respectively, for the *N*-acyl chain and *O*-acyl chain) than that in NPEA (18.16 and 18.25 Å^2, respectively, for the α and β polymorphs) (33). For NMEA, the corresponding value is 19.14 Å^2 (34), which is considerably higher than that observed with DLEA. For DDEA and DMEA, the areas per *N*-acyl chains are 17.99 Å^2 and 18.03 Å^2, which are also slightly lower than the observed values of area per chain in different NAEs. In addition, the packing coefficients of

DAEs are also higher than the respective NAEs with same fatty acyl chainlength. These observations suggest that the higher incremental values of transition enthalpy (ΔH_{inc}), contributed by each methylene unit in the DAEs, are a consequence of the closer chain packing.

It was reported earlier that 1,3-diacylglycerols exhibit higher transition temperature, transition enthalpy, and transition entropy as compared with 1,2-diacylglycerols (36, 47). In 1,2-diacylglycerols, the acyl chains lie side by side and have a hairpin conformation (39, 40), whereas 1,3-diacylglycerols form an extended structure with the two chains separated in a 'V' formation with a dihedral angle of 94° between the two acyl chain planes (36). It was proposed that the V-shape conformation results in a more comfortable chain packing in 1,3-diacylglycerols as compared with 1,2-diacylglycerols (36). In DAEs, the two chains are oriented with respect to each other at an angle of 110–113°, adopting an L-shaped geometry, which may further assist better packing. Our data also support that, compared with hairpin conformation, the lipid molecules pack better in a V- or L-shaped conformation. This may be reflected in higher ΔH_{inc}, ΔS_{inc} for DAEs as compared with NAEs. It may also be noted that transition temperatures of DAEs are higher compared with diacylglycerols of same fatty acyl chainlength, although for the same acyl chains, the latter have higher molecular weights as compared with the former.

CONCLUSIONS

A homologous series *N*-, *O*-diacylethanolamines, which are biologically relevant lipids, were synthesized in this study and their thermotropic phase transitions were characterized by differential scanning calorimetry. A linear dependence was observed in the thermodynamic parameters, ΔH_t and ΔS_t, associated with the chain-melting phase transitions. Crystal structures of three compounds in this lipid series, namely, DDEA, DLEA, and DMEA, were solved by single crystal X-ray diffraction. The structure clearly demonstrates that the conformation of *N*-acyl chain in DAEs is very similar to that found in different NAEs. All the three DAEs adopt an 'L' shape, which may assist better packing with higher ΔH_{inc} values as compared with NAEs. Studies aimed at understanding the interaction of these molecules with other membrane lipids would be expected to provide clues to understand their role in biological membranes. Such studies are currently underway in our laboratory.

REFERENCES

1. Stetten, D., Jr. 1941. Biological synthesis of choline by rats on diets with and without adequate lipotropic methyl. *J. Biol. Chem.* **142:** 629–633.
2. Kewitz, H., and O. Pleul. 1976. Synthesis of choline from ethanolamine in rat brain. *Proc. Natl. Acad. Sci. USA.* **73:** 2181–2185.
3. Schmid, H. H. O., P. C. Schmid, and V. Natarajan. 1990. *N*-Acylated glycerophospholipids and their derivatives. *Prog. Lipid Res.* **29:** 1–43.
4. Chapman, K. D. 2004. Occurrence, metabolism, and prospective functions of *N*-acylethanolamines in plants. *Prog. Lipid Res.* **43:** 302–327.
5. Devane, W. A., L. Hanus, A. Breuer, R. G. Pertwee, L. A. Stevensen, G. Griffin, D. Gibson, A. Mandelbaum, A. Etinger, and R. Mechoulam. 1992. Isolation and structure of a brain constituent that binds to the cannabinoid receptor. *Science.* **258:** 1946–1949.
6. Schuel, H., E. Goldstein, R. Mechoulam, A. M. Zimmerman, and S. Zimmerman. 1994. Anandamide (arachidonylethanolamide), a brain cannabinoid receptor agonist, reduces sperm fertilizing capacity in sea urchins by inhibiting the acrosome reaction. *Proc. Natl. Acad. Sci. USA.* **91:** 7678–7682.
7. Venance, L., D. Piomelli, J. Glowinski, and C. Giaume. 1995. Inhibition of anandamide of gap junctions and intercellular calcium signaling in striatal astrocytes. *Nature.* **376:** 590–594.
8. Facci, L., R. Dal Toso, S. Romanello, A. Buriani, S. D. Skaper, and A. Leon. 1995. Mast cells express a peripheral cannabinoid receptor with differential sensitivity to anandamide and palmitoylethanolamide. *Proc. Natl. Acad. Sci. USA.* **92:** 3376–3380.
9. Chapman, K. D., S. Tripathy, B. Venables, and A. D. Desouja. 1998. *N*-Acylethanolamines: formation and molecular composition of a new class of plant lipids. *Plant Physiol.* **116:** 1163–1168.
10. Akoka, S., C. Tellier, C. LeRoux, and D. Marion. 1988. A phosphorus magnetic resonance and a differential scanning calorimetry study of the physical properties of *N*-acylphosphatidylethanolamines in aqueous dispersions. *Chem. Phys. Lipids.* **46:** 43–50.
11. LaFrance, D., D. Marion, and M. Pézolet. 1990. Study of the structure of *N*-acyldipalmitoylphosphatidylethanolamines in aqueous dispersion by infrared and Raman spectroscopies. *Biochemistry.* **29:** 4592–4599.
12. Swamy, M. J., D. Marsh, and M. Ramakrishnan. 1997. Differential scanning calorimetry of chain-melting phase transitions of *N*-acylphosphatidylethanolamines. *Biophys. J.* **73:** 2556–2564.
13. Ramakrishnan, M., V. Sheeba, S. S. Komath, and M. J. Swamy. 1997. Differential scanning calorimetric studies on the thermotropic phase transitions of dry and hydrated forms of *N*-acylethanolamines of even chainlengths. *Biochim. Biophys. Acta.* **1329:** 302–310.
14. Li, X-M., M. Ramakrishnan, H. L. Brockman, R. E. Brown, and M. J. Swamy. 2002. *N*-Myristoylated phosphatidylethanolamine: interfacial behavior and interaction with cholesterol. *Langmuir.* **18:** 231–238.
15. Kamlekar, R. K., S. Satyanarayana, D. Marsh, and M. J. Swamy. 2007. Miscibility and phase behavior of *N*-acylethanolamine/diacylphosphatidylethanolamine binary mixtures of matched acyl chainlengths (N=14, 16). *Biophys. J.* **92:** 3968–3977.
16. Ramakrishnan, M., R. Kenoth, K. Ravikanth, M. S. Chandra, T. P. Radhakrishnan, and M. J. Swamy. 2002. *N*-Myristoylethanolamine - cholesterol (1:1) complex: first evidence from differential scanning calorimetry, fast-atom-bombardment mass spectrometry and computational modeling. *FEBS Lett.* **531:** 343–347.
17. Kamlekar, R. K., M. S. Chandra, T. P. Radhakrishnan, and M. J. Swamy. 2009. Interaction of *N*-myristoylethanolamine with cholesterol investigated in a Langmuir film at the air-water interface. *Biophys. Chem.* **139:** 63–69.
18. Swamy, M. J., M. Ramakrishnan, D. Marsh, and U. Würz. 2003. Miscibility and phase behaviour of binary mixtures of *N*-palmitoylethanolamine and dipalmitoylphosphatidylcholine. *Biochim. Biophys. Acta.* **1616:** 174–183.
19. Marsh, D., and M. J. Swamy. 2000. Derivatized lipids in membranes: physico-chemical aspects of *N*-biotinyl phosphatidylethanolamines, *N*-acyl phosphatidylethanolamines and *N*-acylethanolamines. *Chem. Phys. Lipids.* **105:** 43–69.
20. Mulder, A. M., and B. F. Cravatt. 2006. Endocannabinoid metabolism in the absence of fatty acid amide hydrolase (FAAH): discovery of phosphorylcholine derivatives of *N*-acyl ethanolamines. *Biochemistry.* **45:** 11267–11277.
21. Han, L., J-R. Gao, Z-M. Li, Y. Zhang, and W-M. Guo. 2007. Synthesis of new plant growth regulator: *N*-(fatty acid) *O*-aryloxyacetyl ethanolamine. *Bioorg. Med. Chem. Lett.* **17:** 3231–3234.
22. Furutani, T., H. Ooshima, and J. Kato. 1997. Preparation of *N*-, *O*-diacylethanolamine from *N*-acylethanolamine using lipase preparations. *Enzyme Microb. Technol.* **20:** 214–220.
23. Marsh, D. 1990. Handbook of Lipid Bilayers. CRC Press, Boca Raton, FL.
24. Sheldrick, G. M. 1997. SHELXL97. Program for the refinement of crystal structures. University of Göttingen, Göttingen, Germany.
25. Casal, H. L., H. H. Mantsch, D. G. Cameron, and R. G. Snyder. 1982. Interchain vibrational coupling in phase II (hexagonal) *n*-alkanes. *J. Chem. Phys.* **77:** 2825–2830.

26. Kodali, D. R., D. Atkinson, and D. M. Small. 1990. Polymorphic behavior of 1,2-dipalmitoyl- 3 -lauroyl(PPl2)- and 3-myristoyl(PP14)-*sn* - glycerols. *J. Lipid Res.* **31:** 1853–1864.
27. Akita, C., T. Kawaguchi, and F. Kaneko. 2006. Structural study on polymorphism of pis-unsaturated triacylglycerol: triolein. *J. Phys. Chem. B.* **110:** 4346–4353.
28. Di, L., and D. M. Small. 1995. Physical behavior of the hydrophobic core of membranes: properties of 1-stearoyl-2-linoleoyl-*sn*-glycerol. *Biochemistry.* **34:** 16672–16677.
29. Larsson, K. 1986. Physical properties–structural and physical characteristics. *In* The Lipid Handbook. F. D. Gunstone, J. L. Harwood, and F. B. Padley, editors. Chapman and Hall, London. 321–384.
30. Ramakrishnan, M., and M. J. Swamy. 1998. Differential scanning calorimetric studies on the thermotropic phase transitions of *N*-acylethanolamines of odd chainlengths. *Chem. Phys. Lipids.* **94:** 43–51.
31. Marsh, D. 1991. Analysis of the chainlength dependence of lipid phase transition temperatures: main and pretransitions of phosphatidylcholines; main and non-lamellar transitions of phosphatidylethanolamines. *Biochim. Biophys. Acta.* **1062:** 1–6.
32. Marsh, D. 1982. Biomembranes. *In* Supramolecular Structure and Function. G. Pifat and J. N. Herak, editors. Plenum Press, New York. 127–178.
33. Kamlekar, R. K., and M. J. Swamy. 2006. Molecular packing and intermolecular interactioms in two structural polymorphs of *N*-palmitoylethanolamine, a type-2 cannabinoid receptor agonist. *J. Lipid Res.* **47:** 1424–1433.
34. Ramakrishnan, M., and M. J. Swamy. 1999. Molecular packing and intermolecular interactions in *N*-acylethanolamines: crystal structure of *N*-myristoylethanolamine. *Biochim. Biophys. Acta.* **1418:** 261–267.
35. Dahlén, B., I. Pascher, and S. Sundell. 1977. The crystal structure of *N*-(2-hydroxyethyl)-octadecanoate. *Acta Chem. Scand. A.* **31:** 313–320.
36. Goto, M., K. Honda, L. Di, and D. M. Small. 1995. Crystal structure of a mixed chain diacylglycerol, 1-stearoyl-3-oleyl-glycerol. *J. Lipid Res.* **36:** 2185–2190.
37. Dahlén, B., and I. Pascher. 1972. Molecular arrangements in sphingolipids. Crystal structure of *N*-tetraeosanoylphytosphingosine. *Acta Crystallogr. B.* **28:** 2396–2404.
38. Hindenes, J-O., W. Nerdal, W. Guo, L. Di, D. M. Small, and H. Holmsen. 2000. Physical properties of the transmembrane signal molecule, *sn*-1-stearoyl 2-arachidonoylglycerol. Acyl chain segregation and its biochemical implications. *J. Biol. Chem.* **275:** 6857–6867.
39. Pascher, I., S. Sundell, and H. Hauser. 1981. Glycerol conformation and molecular packing of membrane lipids. The crystal structure of 2,3-dilauroyl-D-glycerol. *J. Mol. Biol.* **153:** 791–806.
40. Han, G. W., J. R. Ruble, and B. M. Craven. 1994. The crystal structure of 1,2-dipalmitoyl-sn-glycerol at 123 K. *Chem. Phys. Lipids.* **71:** 219–228.
41. Abrahamsson, S., B. Dahlén, H. Löfgren, and I. Pascher. 1978. Lateral packing of hydrocarbon chains. *Prog. Chem. Fats Other Lipids.* **16:** 125–143.
42. Maulik, P. R., M. J. Ruocco, and G. G. Shipley. 1990. Hydrocarbon chain packing modes in lipids: effect of altered sub-cell dimensions and chain rotation. *Chem. Phys. Lipids.* **56:** 123–133.
43. Alkorta, I., I. Rozas, and J. Elguero. 1998. Non-conventional hydrogen bonds. *Chem. Soc. Rev.* **27:** 163–170.
44. Desiraju, G. R. 1996. The C-H···O hydrogen bond: structural implications and supramolecular design. *Acc. Chem. Res.* **29:** 441–449.
45. Blatchford, M. A., P. Raveendran, and S. L. Wallen. 2000. Raman spectroscopic evidence for cooperative C−H···O interactions in the acetaldehyde-CO complex. *J. Am. Chem. Soc.* **124:** 14818–14819.
46. Chang, H-C., J-C. Jiang, C-W. Chuang, and S. H. Lin. 2004. Evidence for hydrogen bond-like C–H–O interactions in aqueous 1,4-dioxane probed by high pressure. *Chem. Phys. Lett.* **397:** 205–210.
47. Kodali, D. R., D. A. Fahey, and D. M. Small. 1990. Structure and polymorphism of saturated monoacid 1,2-diacyl-sn-glycerols. *Biochemistry.* **29:** 10771–10779.